

ORIGINAL ARTICLE

Femoral arteries energy dissipation and filtering function remain unchanged after cryopreservation procedure

Daniel Bia,¹ Yanina Zócalo,¹ Franco Pessana,² Ricardo Armentano,^{1,2} Héctor Pérez-Campos,³ María Saldías³ and Inés Álvarez³

1 Facultad de Medicina, Department of Physiology, Universidad de la República, Montevideo, Uruguay

2 Facultad de Ingeniería y Ciencias Exactas y Naturales, Universidad Favaloro, Buenos Aires, Argentina

3 Facultad de Medicina, Unidad de Criobiología, Instituto Nacional de Donación y Transplante de Células, Tejidos y Órganos (Ex. BNOT) MSP, Montevideo, Uruguay

Keywords

arterial wall, cryopreservation, femoral arteries, organ preservation and procurement, pressure–diameter, techniques, tissue banking, tissue transplantation, vessels, viscoelasticity.

Correspondence

Prof. Daniel Bia, Researcher, Physiology, School of Medicine, General Flores 2125, Montevideo 11800, Uruguay. Tel.: 0598 2 9243414; fax: 0598 2 9240395; e-mail: dbia@fmed.edu.uy

Received: 2 June 2005

Revision requested: 12 July 2005

Accepted: 28 August 2005

doi:10.1111/j.1432-2277.2005.00220.x

Summary

The aim was to evaluate our cryopreservation method effects on the mechanical properties and filtering function of human superficial femoral arteries (SFA). SFA segments from 10 multiorgan donors were divided into two groups: *fresh*, tested 24–48 h after harvesting, and *cryopreserved/defrosted*, tested after 1 month of cryopreservation. The cooling process was carried out in three steps: 2 °C/min until –40 °C; 5 °C/min until –90 °C and finally a rapid cooling by transferring the bag to vapour phase of liquid nitrogen (–142 °C). Thawing was made in two steps, a slow warming time by exposing the bag to 20 °C during 20 min, followed by a rapid warming by immersion in a 40 °C warm bath until defrost. In a circulation mock, arterial pressure [*Pressure signal (P)*] and diameter [*Diameter (D)*] were registered at similar stretch-frequency, *P* and flow levels. A compliance transfer function (*D/P*) was used for the on-line assessment of the arterial wall elastic (*E*), viscous (η), and inertial (*M*) properties. To evaluate the arterial wall filter function, the arterial wall *D/P* frequency response was characterized, the cut-off frequency (f_c) was quantified, and the viscous energy dissipation (W_η) was calculated. After cryopreservation, there were not significant changes in *E*, η , *M*, W_η , and f_c .

Introduction

Arteries are categorized into two broad types: elastic (i.e. aorta, common carotid) and muscular (i.e. femoral, coronaries) arteries. In an histological approach, the medial layer of both, elastic and muscular arteries, is composed by the same principal components – smooth muscle, elastin and collagen fibres – but, the amount and fraction of these components and the wall organization vary, according to the arterial type and the anatomic location [1]. Additionally, the categorization in elastic and muscular arteries is based not only on structure, but also on their different physiological role. The elastic arteries are distinguished by their tiny

elasticity and viscosity [2]. This helps them smooth out the large fluctuations in pressure and flow determined by the heartbeat [2,3]. During systole, the elastic sheets are stretched, minimizing the peak of systolic blood pressure and the ventricle after load; during diastole, the elastic rebound helps maintain elevated mean and diastolic arterial pressures, and the mean blood flow [2,3]. In contrast, the muscular arteries are characterized by their larger elasticity and viscosity, and the predominant constituent of the tunica media is the smooth muscle [1,2]. The main role of muscular arteries is to distribute blood throughout the body and to produce an important smooth muscle-dependent energy dissipation in order to cushion the pressure and flow

pulsatility [2,3]. In summary, it could be said that the arterial wall viscoelastic behaviour allows an efficient transmission of blood to the peripheral tissues (conduit function, CF), at the time pressure and flow fluctuations are dampened (filter function) [2–4]. Additionally, the arterial elasticity avoids wall's over-distension because of pressure, giving structural security to the arterial segment [2–4]. Unfortunately, venous and commercially available prosthetic vascular grafts do not reproduce these physiological and favourable characteristics. In fact, they have shown to be stiffer than arteries during arterial haemodynamic conditions. The implantation of a stiffer vein or synthetic graft into the arterial tree diminishes the perfusion and buffering efficiency [5]. Additionally, the mismatch in viscoelastic properties between the graft and native artery has been related to the graft failure [5,6]. To reduce the viscoelastic mismatch between the prosthesis and the native artery, an interesting alternative would be the use of an autologous artery, as the vascular graft. About this, the human superficial femoral artery has been used in clinical works [7,8]. However, except in certain limited surgeries (i.e. coronary bypass), it is difficult to obtain an autologous artery of adequate length and size without the sacrifice of an organ or essential part. In the lack of suitable autologous materials, an alternative would be the use of cryopreserved/thawed arteries [9,10]. In this way, cryopreservation has become an important tool for the storage of human cardiovascular tissues.

However, it has been demonstrated that the post-thaw functional recovery of cryopreserved blood vessels could be associated with an impaired biomechanical performance [11]. Nevertheless, study results are controversial, and at date the effects of cryopreservation on mechanical properties of human arteries remain unclear. Among the factors that contribute to this undefined issue are the different degrees of tolerance to cryopreservation that elastic and muscular arteries express because of their different structural composition [12,13]. Recently, we demonstrated that the techniques of cryopreservation used in our tissue bank do not significantly affect the mechanical behaviour of human common carotids (elastic arteries) in any detrimental way [14]. However, the effect of cryopreservation on human SFA viscoelasticity, inertia and functional properties remains to be established.

In this context, the aim of this work was to evaluate the effects of our cryopreservation technique on muscular arteries biomechanical properties and filter function. To fulfil the aim, the biomechanical properties of fresh and cryopreserved/thawed SFA were analysed in an *in vitro* system, and contrasted at identical pressure, flow and stretch-frequency levels [4,14,15].

Materials and methods

Donor criteria selection

All procedures took into account ethical and safety concerns for therapeutic use, and include consent documentation according to No. 14005 and No. 17668 legal rulers of República Oriental del Uruguay. General and particular exclusion criteria for vascular tissue procurement were taken in accordance with the International Atomic Energy Agency (IAEA, International Standards for Tissue Banks), American Association Tissue Banking (AATB) and European Association Tissue Banking (EATB).

Tissue procurement

The SFAs used in this work were procured from 10 donors in brain death condition, during multiple organ and tissue harvesting, under Banco Nacional de Organos y Tejidos transplant program from República Oriental del Uruguay [16]. Donors age was 30 ± 6 years.

Segments from both right and left SFA were harvested. Aseptic cleaning on the Scarpa's triangle region with 7% povidone–iodine solution was made after aortic clamp and cardiac arrest. Sterile drapes were used to establish surgical field. Under aseptic conditions, a 7-cm segment of SFA was cleared from surrounding tissues. In all cases, *in situ* SFA measurements of 5-cm long were performed and two suture references were placed in the vessel adventitia. After harvesting, the segments were washed with saline solution and stored at 4 °C in a saline solution (NaCl 0.9 g%) with gentamicine (16 mg%), cefuroxime (300 mg%), penicillin G (400.000 IU%), and fluconazol (8 mg%). The warm ischaemia time was 53–67 min (Mean = 61 min), and the cold ischaemia was 24–48 h (Mean: 34 h). For each donor, an arterial segment was assigned to the fresh-control group and the other to the cryopreserved/thawed group. After 24–48 h, segments corresponding to fresh-controls were sent for *in vitro* mechanical tests. Segments from the cryopreserved/thawed group were subjected to the cryopreservation procedure.

Cryopreservation procedure

After incubation in saline and antibiotic solution, the samples were placed in a sterile bag (volume: 350 cc) containing 85 cc of cryopreservant solution: Culture Medium (RPMI 1640): 85%; Human Albumin Solution (20%): 5%; and Dimethylsulfoxide (DMSO): 10% [17,18]. In a laminar flow cabinet (Microflow, Laminar Flow Work Station, MDH Ltd, Wal Worth Road Andover Hants England SP.10.5.AA), the bag was sealed hermetically at vacuum (Joisten and Kettenbaum, D51429, Ber-eisch Gladbach, Mod.011342) and was equilibrated for

30 min at 20 °C. After that, the programmed cryopreservation was carried out in a Controlled Rate Freezing System (Model 9000, Gordinier Electronics, Inc. 29975 Parkway, Roseville, MI 48066, USA).

For the cooling process, we chose a modified protocol from Pegg's *et al.* [19]. It consisted in three operative time steps. Firstly, a slow programmed cooling rate with a mean value of 2 °C/min until -40 °C. Secondly, a slow programmed cooling rate with a mean value of 5 °C/min until -90 °C. Thirdly, a rapid cooling rate obtained by the transference of the bag to the gaseous phase of the liquid nitrogen compartment (-142 °C). The frozen arterial specimens were stored for 30 days at -142 °C (Mark III, Temperature and Liquid Level Controller, Taylor, Wharton, Theodore, AL, USA). After the storage period, vessels were defrosted. In our standard warming protocol, a two-stage process was used, also taking into account Pegg *et al.* works [19], which highlight the importance of the thawing rate, in order to avoid the fractures [19–21]. The thawing protocol first step was a slow process, achieved by transferring the bag from the nitrogen gaseous phase to room temperature (20 °C) during 30 min. Then, during the second step, the bag was rapidly transferred to a 40 °C water bath until completely defrost. After thawing, to prevent osmolar stress, the cryoprotectant solution was gradually removed in four 10 min-steps by the immersion in tapered concentrations

(10, 5, 2.5, and 0% of DMSO) at 20 °C. The cryoprotectant removal total time was 40 min [18]. Finally, the arterial segments were sent, immersed in saline solution (NaCl 0.9 g%) to be mechanically tested.

In vitro mechanical tests

To perform the mechanical tests, each arterial segment was nontraumatically mounted (at *in vivo* length) on specifically designed cannulas of the flow circuit loop (Fig. 1). A full description of this device has been published previously [6,14,22]. Once mounted, the segment remained immersed and perfused with a thermally regulated (37 °C), oxygenated Tyrode's solution, with pH = 7.4 [2,6,14,22]. The perfusion line was powered by a pneumatic pump (PP) (Jarvik Model 5, Kolff Medical Inc., Salt Lake City, UT, USA). The pneumatic device was regulated by an air supply machine that allowed adjustments of the pump rate, pressure and flow values, and waveforms [2,6,14,22].

To measure the arterial pressure, each segment was instrumented with a pressure micro transducer (1200 Hz frequency response, Konigsberg Instruments, Inc., Pasadena, CA, USA) inserted in the vessel through a stab wound. To measure arterial external diameter, a pair of ultrasonic crystals (5 MHz, 2 mm diameter) was sutured to the arterial adventitia. The transit time of the ultrasonic signal (1580 m/s) was converted into distance

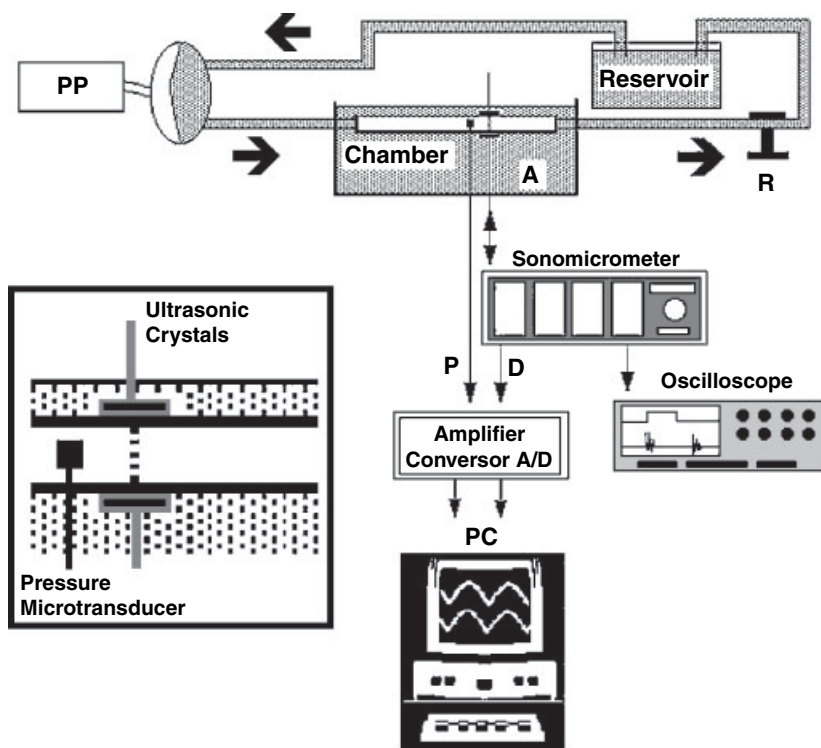


Figure 1 Circulating loop showing a PP and a perfusion line with a chamber, a resistance modulator (R) and a reservoir. Tyrode's solution is thermally controlled (A). Pressure signal (P) is obtained using a solid transducer, and diameter (D) signals are obtained using a pair of ultrasonic crystals and a sonomicrometer. All signals are monitored on an oscilloscope and stored in a personal computer (PC).

by means of a sonomicrometer (1000 Hz frequency response, Triton Technology Inc. San Diego, CA, USA). Optimal positioning of the dimensional gauges was assessed by an oscilloscope (model 465B; Tektronix, Richardson, TX, USA).

Once instrumented, the arterial segments were allowed to equilibrate for 10 min under a steady state of flow and mean pressure.

Data acquisition

After the equilibration time, a similar protocol was followed for the fresh and cryopreserved/thawed segments, in order to characterize their mechanical properties. Diameter and pressure waves were measured under the dynamic conditions, displayed in real time, digitized every 5 ms and stored for off-line analysis in the computer hard disk. Approximately, 20–30 consecutive beats were sampled and analysed.

Flow, pressure and stretching rate levels similar to the observed in normotensive patients were chosen. Recordings were carried out submitting the segments to a stretching rate of ~65 cycles/min, an intravascular pulse pressure of ~65 mmHg and mean pressure of ~85 mmHg, and a mean flow of ~250 ml/min. In all cases, the pump, and tubing resistance were regulated so as to generate adequate pressure waveforms (Fig. 2).

Data analysis

A computerized procedure was used to determine the pressure–diameter loop and to calculate the biomechanical parameters using an original system developed in our laboratory [14,15,23]. A linear autoregressive, with exogenous input model (ARX) was used to fit the data. The general discrete time ARX model is given by:

$$D[k] = - \sum_{j=1}^{n_y} a_j D[k-j] + \sum_{i=0}^{n_x} b_i P[k-i] \quad (1)$$

where D is the estimated diameter, P the segment pressure, a_j and b_i are the coefficients to be estimated from the measured data. The value of n_x and n_y defines the model order. The ARX model was applied to the input–output (pressure–diameter) data to assess the arterial dynamics. In this way, the arterial diameter is estimated from the input of the model using the identified coefficients a_j and b_i . The parameters for each model fit were estimated using the least square algorithm [24].

As a special case of the general model (1), we considered a third-order model. This model was chosen as the mean order model using the Akaike information criterion (AIC) statistic [25] over the whole population. Considering the estimated coefficient $\{a_j, j = 1, \dots, 3\}$ and $\{b_i, i = 0, \dots, 3\}$, the general transfer function in the z -transform domain is:

$$H(z) = \frac{D(z)}{P(z)} = \frac{b_0 + b_1 z^{-1} + b_2 z^{-2} + b_3 z^{-3}}{1 + a_1 z^{-1} + a_2 z^{-2} + a_3 z^{-3}} \quad (2)$$

Inverse bilinear transformation was applied to (2), in order to obtain a continuous transfer function (from the z -plane to the s -plane):

$$H_a(s) = \frac{m_3 s^3 + m_2 s^2 + m_1 s + m_0}{n_3 s^3 + n_2 s^2 + n_1 s + n_0} \quad (3)$$

From this third-order model, the dynamic range (corner frequency, f_c) was determined taking into account its half-power point, corresponding to -3 dB down from its low frequencies value (Fig. 3). The elimination of the

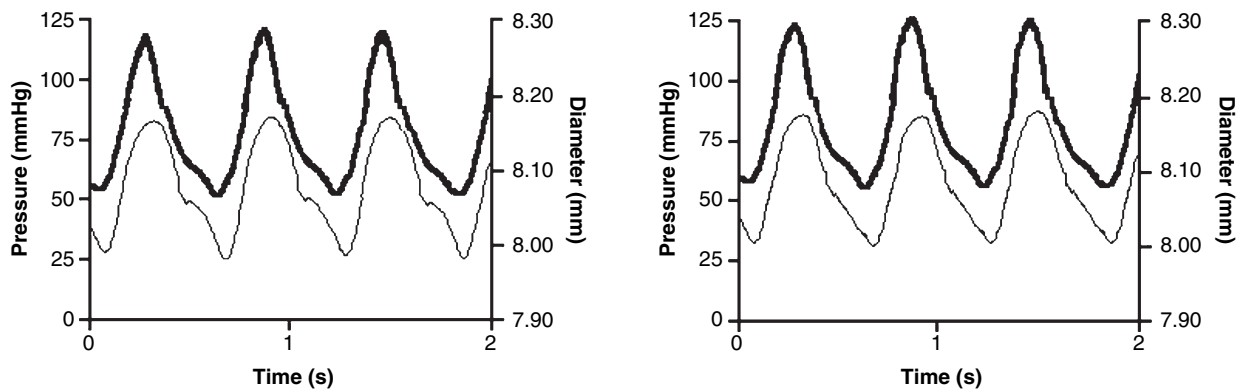


Figure 2 *In vitro* pressure (thick line) and diameter (thin line) signals obtained in a fresh SFA (left) and a cryopreserved/thawed SFA (right), to come from the same multiorgan donor.

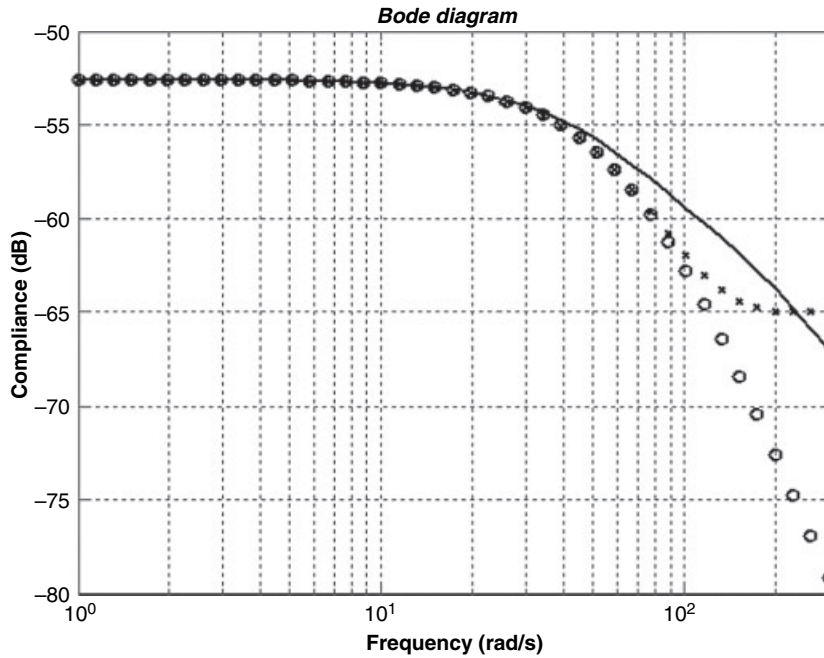


Figure 3 Solid line: absolute Bode plot of the third-order approximation $H_a(\omega)$. Crosses: absolute Bode plot of the second-order approximation $H_b(\omega)$. Circles: absolute Bode plot of the physiological model $H_c(\omega)$.

highest frequency parameters (m_3 and n_3) did not introduce notable differences in the physiological frequency range of the transfer function $H_a(s)$. The model reduction is:

$$H_b(s) = \frac{m_2s^2 + m_1s + m_0}{n_2s^2 + n_1s + n_0} \quad (4)$$

To give physiological meanings to the coefficients, m_2 and m_1 were neglected and the model was readjusted to:

$$H_c(s) = \frac{m_0}{n_2s^2 + n_1s + n_0} \quad (5)$$

In the continuous time domain, the model is better understood and a physical meaning can be given to the model coefficients. These coefficients are related to a linear time invariance ordinary differential equation. Assuming a second-order differential equation to characterize wall dynamics, the frequency response of (5) would be [26]:

$$H_c(s) = \frac{D(s)}{P(s)} = \frac{1}{Ms^2 + \eta s + E} \quad (6)$$

From (5) and (6), we resume the elastic ($E = n_0/m_0$), viscous ($\eta = n_1/m_0$) and inertial ($M = n_2/m_0$) indexes. Figure 3 shows the relationship between transfer functions (3), (4) and (5) that reinforces our wall transfer function approximation and their similarity in the physiological

ranges of the angular frequency ω . In this figure, we can observe the frequency response of the ARX model given by (3) i.e. $H_a(\omega)$, the frequency response of the second-order system $H_b(\omega)$ and the frequency response of an arterial wall segment $H_c(\omega)$.

The arterial wall, modelled as a second-order mechanical system (6), could be associated to a low-pass filter (Fig. 3), which corner frequencies (f_{c1} and f_{c2}) were calculated as [26]:

$$f_{c1,2} = \frac{1}{2\pi} \left[\frac{\eta}{2M} \pm \sqrt{\left(\frac{\eta}{2M}\right)^2 - \frac{E}{M}} \right] \quad (7)$$

Assuming that f_{c2} (related to inertial effects) is larger than f_{c1} , we can accept that $2 \times \pi \times f_{c1}$ is the dominant pole of the transfer function $H_b(\omega)$. Consequently, the first-order system obtained from our model reduction, coincide with other arterial models that represent the arterial wall mechanics [26]. Taking into account this reduction, the dynamic range of the low-pass filter would have the dynamical range:

$$f_{c1} = \frac{1}{2\pi} \frac{E}{\eta} \quad (8)$$

with $1/E$ the flat amplitude in the band pass (low frequencies) of the compliance (diameter/pressure) frequency response.

Finally, the arterial wall viscous energy dissipation by cardiac or pump cycle (W_η) was computed as [27]:

$$W_{\eta} = 4 \times \omega \times \eta \times A \quad (9)$$

where ω is the angular frequency [$2 \times \pi \times$ pump rate], W_{η} represents loss modulus of the complex elastic modulus, [3] and A is the mean cross-sectional area.

Statistical analysis

Values were expressed as mean values \pm standard deviation (MV \pm SD). Model order selection was obtained using the AIC [25]. To evaluate the nature of the error of the ARX model fitting procedure, correlation and residual analysis was performed. Frequency response comparisons between fresh and cryopreserved/defrosted arteries were made at each physiological frequency level, using a two-tailed unpaired Student's *t*-test. The haemodynamic and mechanical data comparisons were performed using a two-tailed unpaired Student's *t*-test. Differences of $P < 0.05$ were considered significant.

Results

Physiological waveforms, with their harmonic content, and pressure levels were simulated in the mock system (Fig. 2; Table 1). Pressure and frequency levels were similar between both groups, allowing to perform an isobaric and isofrequency analysis. It is also to note that the arterial diameter did not change after cryopreservation (Table 1).

Figure 3 shows the compliance transfer function response of the SFA wall in the frequency domain. A low-pass filter response was observed. As Fig. 3 shows, in the physiological ranges, the frequency response of the three transfer functions, at each frequency level, was not different, allowing the proposed order reduction. The arterial wall mechanical properties can be represented by three main indexes that characterize the elastic, viscous and inertial behaviour. Accordingly, a second-order model was used to reduce the order model, $H_b(s)$ and the numerator coefficients were neglected, preserving the physiological meaning of the second-order differential equation, $H_c(s)$.

Table 1. Haemodynamic parameters.

	Fresh arteries ($n = 10$)	Cryopreserved/defrosted arteries ($n = 10$)
Systolic pressure (mmHg)	130 \pm 7	131 \pm 8
Diastolic pressure (mmHg)	66 \pm 6	67 \pm 5
Mean pressure (mmHg)	86 \pm 7	89 \pm 5
Mean diameter (mm)	7.20 \pm 0.94	7.24 \pm 0.82
Pump rate (Hz)	1.10 \pm 0.07	1.10 \pm 0.10

Mean \pm SD values.

Figure 4 shows the wall frequency response of the compliance transfer function $H_a(\omega)$ for both groups, with their confidence interval. Note that the cryopreserved/defrosted arteries rely within the fresh range showing no significant differences between the groups.

Table 2 shows the biomechanical and functional indexes. Note that fresh and cryopreserved/defrosted segments did not show significant differences in their elastic, viscous and inertial indexes. Additionally, there were differences neither in the filter function nor in the viscous energy dissipation, between fresh and cryopreserved/defrosted arteries.

Discussion

Several methodological aspects should be considered so as to perform an appropriate biomechanical evaluation that allows obtaining functional information of the arterial grafts. Although static analyses (i.e. incremental stress-strain test) allow the indirect evaluation of frequency-dependent mechanical properties [28,29], an adequate characterization of the functional meaning and contribution of this properties requires a dynamic analysis, in which the arterial wall is submitted to conditions similar to real haemodynamic situations. Consequently, we did an isobaric, isofrequency, and dynamic study [2,4,14,15,23]. We opted for arterial segments, instead of the most commonly used blades or rings, because the former has shown to be better to preserve the shape and integrity of the arterial wall [30,31].

A parametric system identification approach was achieved to calculate the vessels mechanical parameters (compliance Bode plot) [23]. Such procedure characterizes the pressure–diameter hysteresis loop by estimation of the viscoelastic behaviour of the vessel wall dynamics providing their individual contribution. This adaptive procedure has been previously employed *in vitro* in human carotid arteries [14]. An initial third-order model was chosen. A low-pass response was observed in the transfer function, representing the compliant response of the vessel wall in the frequency domain (Bode plot). The vessel wall can be described using three main parameters that resume the elastic, viscous and inertial behaviours, respectively. Accordingly, a second-order simplification was tested. Finally, the numerator coefficients were neglected to preserve the physiological correlation of its second-order differential equation, more suitable for clinical purpose. The three types of compliance Bode plots tested *in vitro* did not show differences in the physiological range (Fig. 3).

During cryopreservation, several damages to the cellular (i.e. smooth muscle cells) and extra-cellular (i.e. elastin and collagen fibres) constituents of the arterial wall

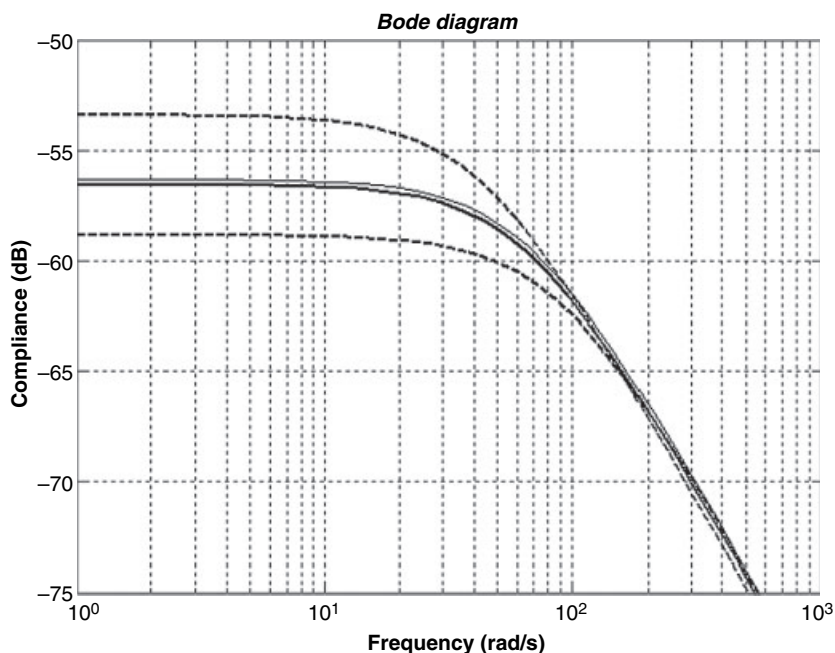


Figure 4 Thick Line: Mean third-order model $H_a(\omega)$ for fresh arteries. Thin line: Mean cryopreserved third-order model $H_a(\omega)$. Dash line: Mean values \pm SD of $H_a(\omega)$ for fresh arteries. Cryopreserved frequency response was placed inside the fresh (95%) confidence interval.

Table 2. Biomechanical and functional parameters.

	Fresh arteries ($n = 10$)	Cryopreserved/thawed arteries ($n = 10$)
E (mmHg/mm)	670.90 ± 68.24	664.09 ± 71.08
η (mmHg·s/mm)	17.23 ± 3.35	17.13 ± 2.93
M (10^{-1}) (mmHg·s ² /mm)	1.88 ± 0.23	1.89 ± 0.20
W_{η} (10^4) (mmHg/s)	1.05 ± 0.23	1.05 ± 0.22
f_c (Hz)	10.34 ± 1.61	10.46 ± 1.46

Mean \pm SD values. E , η and M : elastic, viscous and inertial indexes; W_{η} : viscous energy; f_c : corner frequency.

have been described [11,12,32,33]. The damage has been related to many factors such as the cooling and thawing rate, temperature range and cryoprotectant toxicity. The deleterious effects of the different factors have been ascribed to mechanic, osmotic, biochemical and thermal stresses that build up during cryopreservation [18–21,32,33]. These factors were considered, and our technique of cryopreservation is in agreement with the techniques, which have shown the best results [19–21,32,34].

The structural impairment of the arterial wall during cryopreservation could determine alterations in the arterial viscoelasticity and functional capability, as this depends on the arterial wall cellular and extra-cellular components. About this, the arterial elastic behaviour at low strains has been attributed mainly to the elastin fibres, while the collagen fibres are the chief responsible for that behaviour at high strain. The vascular smooth muscle has been proposed to contribute to elasticity at intermediate strains [15]. Our results show that there

were no differences in the elastic level before and after cryopreservation. This is in accordance with results referred by Rosset *et al.* [12] who found that after cryopreservation of human SFA, there were no changes in the arterial stiffness. Additionally, Blondel *et al.* [35] performing *in vitro* inflation static tests on SFA segments found nonsignificant differences between the incremental elastic and pressure–strain modulus of fresh and cryopreserved segments. However, in Blondel's work, differences between fresh and cryopreserved arteries were observed when other mechanical parameters (i.e. wall stiffness) were calculated [35].

The viscosity of the vascular wall, usually associated to an energy dissipation term [2,4,15,29,36], helps attenuate travelling pressure pulses along the arteries, and prevents reflected pressure waves from resonating in the arterial system [37]. Passive theories propose that wall viscosity is a property of the vascular wall cellular constituents, and a higher viscosity has been reported in vessels with a higher content of smooth muscle cells [2,4,15,38]. An additional important factor is the collagen-dependent viscosity [29,39,40]. Classically, collagen has been considered of minor, or null importance in the wall viscosity. However, collagen fibres, particularly type III, which are present in the arterial wall, could contribute to the arterial wall viscous behaviour, as the loading of collagen has shown to result not only in elastic energy storage, by stretching the flexible molecular domains, but also in energy dissipation by fibrillar slippage [29,39,40]. On the other hand, active theories propose that viscosity depends on smooth muscle tone. The viscosity increase during smooth muscle activa-

tion supports these theories [2,4,15,38]. Anyway passive and active theories are not mutually excluded.

Our results show that after cryopreservation, this important dynamic property is preserved.

Rigorously speaking, the inertial index is a proportionality constant between force and the acceleration developed by a given material, and quantifies a body resistance to acceleration. In arterial wall dynamics, inertial forces might develop at the beginning of systole, associated to the fast increase in diameter [15], and the main determinant of the arterial wall inertia is the wall mass [15]. Our results show that inertia did not change after cryopreservation. In consequence, the functional role of the arterial wall mass was not altered after cryopreservation.

The inertia of the wall mass, even including the effective mass from the surrounding soft tissues, is negligible compared with the elastic and viscous force because of low wall velocities [36]. However, as it is a determinant of the mechanical behaviour, it is required in order to characterize the third-order model approximation of the wall [14,23]. Nevertheless, the similarity among the three Bode plots of the wall transfer functions in the physiological range observed in Fig. 3 allowed the use of the corner frequency of a first-order model, f_{c1} (which does not take into account the inertial effect), to characterize the wall dynamic range (i.e. corner frequency, -3 dB point in the vessel compliance frequency response).

The arterial wall filtering function, that is to say the capability of the arterial wall to store, transmit, and dissipate energy, is the key to the supplementary pumping action of the arterial wall, as well as to prevent early mechanical failure or disruption of the arterial wall components [4,36]. As a law, high frequency vibrations produce structure injuries, and the aim of filtering is to reduce accelerated oscillations. The filter function is inversely related to the corner frequency (-3 dB Bode plot), which represents the limit of frequencies that are not filtered (dynamic range) by the arterial wall; so, a quantitative measure of arterial filter function can be obtained by using the corner frequency (f_c) [14]. Our results showed a similar f_c between fresh and cryopreserved/defrosted arteries (Table 2). This can be clearly observed in Fig. 4, which shows that cryopreserved/defrosted segments frequency response is included in the confidence interval of the fresh-control group. Additionally, the amplitude at low frequencies of the compliance (pressure–diameter) frequency response (related with $1/E$) was similar in both groups of arteries (Fig. 4). In consequence, it could be said that the arterial wall low-pass filter function is preserved after cryopreservation.

A complementary mechanical approach to evaluate the filter function implies considering the conversion of mechanical energy into thermal energy in the arterial wall

[3,41]. The arterial wall dissipates energy in order to avoid the transference of the high frequency components of the pressure wave to vascular diameter, exerting a protective effect on the arterial wall. The viscous energy dissipation, measured at a cross-sectional level, although appearing small in absolute value, may be much higher if it is integrated all along the arterial tree. We found no differences in the viscous energy dissipation between fresh and cryopreserved arteries. Consequently, this results support that the arterial wall filter performance remained unchanged after cryopreservation.

An important consideration should be mentioned about the practical relevance of our results. Nowadays, improving organ and tissue preservation techniques for transplantation is still one of the most important goals of transplantation research. Until now, there is not a standard methodology of cryopreservation that ensures good results, and several controversies remain about numerous aspects of cryopreservation: the best cryosolution, the optimal cooling and thawing rates, the temperature range that should be used, etc. Additionally, the evaluation of the cryopreservation effects on the arterial wall mechanical properties has shown controversial results [11,12,35]. In this context, it was important to evaluate the effects of our cryopreservation method on the mechanical and functional properties of SFA homografts. It should be noted that *in vitro* studies provide no insight into the degree of function that the tissue is capable of *in vivo*, and a good or bad performance may either be repaired or aggravated following transplantation. However, *in vitro* studies have substantial value for the optimization of cryopreservation techniques, and have been extensively used for this purpose [11,12,35,42]. In such studies, factors that could affect the mechanical properties of the arteries after implantation (i.e. the immune response) are eliminated. So, if we are thinking to use the cryopreserved vessels as vascular substitutes or scaffolds, a complete *in vitro* biomechanical and functional evaluation would be necessary as a first experimental step. However, only *in vivo* postimplanted studies would give information related to the SFA homograft clinical utility. Additionally, to completely understand the cause/s of the cryopreserved artery failure, *in vivo* postimplantation studies are also necessary. In this sense, *in vitro* and *in vivo* studies give complementary data.

In summary, no statistical differences were found between the dynamic biomechanical behaviour of cryopreserved/defrosted and fresh SFA. Moreover, the SFA wall filter function was preserved after cryopreservation. We can conclude that our cryopreservation technique allows the banking of human SFA preserving its biomechanical and functional behaviour, offering vascular grafts for cardiovascular and peripheral surgery, with bio-

mechanical and functional properties similar to the fresh SFA homografts.

Acknowledgements

The authors gratefully acknowledge the technical assistance of Mr Elbio Agote and the personnel of tissue bank.

References

- Fawcett DW. Sistemas vasculares sanguíneo y linfático. In: Fawcett DW, ed. *Textbook of Histology*, Bloom-Fawcett, 11th edn. Interamericana: McGraw-Hill, 1986: 150–187.
- Bia D, Aguirre I, Zocalo Y, Devera L, Cabrera Fischer E, Armentano R. Regional differences in viscosity, elasticity and wall buffering function in systemic arteries: pulse wave analysis of the arterial pressure-diameter relationship. *Rev Esp Cardiol* 2005; **58**: 167.
- Nichols WW, O'Rourke MF. *McDonald's Blood Flow in Arteries. Theoretical, Experimental and Clinical Principles*, 4th edn. London, UK: Edward Arnold, 1998.
- Bia D, Barra JG, Grignola JC, Gines FF, Armentano RL. Pulmonary artery smooth muscle activation attenuates arterial dysfunction during acute pulmonary hypertension. *J Appl Physiol* 2005; **98**: 605.
- Tai NR, Salacinski HJ, Edwards A, Hamilton G, Seifalian AM. Compliance properties of conduits used in vascular reconstruction. *Br J Surg* 2000; **87**: 1516.
- Cabrera EI, Bia D, Cassanello GL, *et al.* Reduced elastic mismatch achieved by interposing vein cuff in expanded polytetrafluoroethylene femoral bypass decreases intimal hyperplasia. *Artif Organs* 2005; **29**: 122.
- Sessa CN, Morasch MD, Berguer R, Kline RA, Jacobs JR, Arden RL. Carotid resection and replacement with autogenous arterial graft during operation for neck malignancy. *Ann Vasc Surg* 1998; **12**: 229.
- Fields CE, Bower TC. Use of superficial femoral artery to treat an infected great vessel prosthetic graft. *J Vasc Surg* 2004; **40**: 559.
- Albertini JN, Barral X, Branchereau A, *et al.* Long-term results of arterial allograft below-knee bypass grafts for limb salvage: a retrospective multicenter study. *J Vasc Surg* 2000; **31**: 426.
- Pascual G, Jurado F, Rodriguez M, *et al.* The use of ischemic vessels as prostheses or tissue engineering scaffolds after cryopreservation. *Eur J Vasc Endovasc Surg* 2002; **24**: 23.
- Rigol M, Heras M, Martinez A, *et al.* Changes in the cooling rate and medium improve the vascular function in cryopreserved porcine femoral arteries. *J Vasc Surg* 2000; **31**: 1018.
- Rosset E, Friggi A, Novakovitch G, *et al.* Effects of cryopreservation on the viscoelastic properties of human arteries. *Ann Vasc Surg* 1996; **10**: 262.
- Arnaud F. Endothelial and smooth muscle changes of the thoracic and abdominal aorta with various types of cryopreservation. *J Surg Res* 2000; **89**: 147.
- Bia D, Pessana F, Armentano R, *et al.* Cryopreservation procedure does not modify human carotid homografts mechanical properties: an isobaric and dynamic analysis. *Cell Tissue Bank* 2005 (in press).
- Armentano RL, Barra JG, Levenson J, Simon A, Pichel RH. Arterial wall mechanics in conscious dogs. Assessment of viscous, inertial, and elastic moduli to characterize aortic wall behavior. *Circ Res* 1995; **76**: 468.
- Alvarez I, Del Carmen Saldias M, Wodowoz O, *et al.* Progress of National Multi-tissue Bank in Uruguay in the International Atomic Energy Agency (IAEA) Tissue Banking Programme. *Cell Tissue Bank* 2003; **4**: 173.
- Fahy GM, Lilley TH, Linsdell H, Douglas MS, Meryman HT. Cryoprotectant toxicity and cryoprotectant toxicity reduction: in search of molecular mechanisms. *Cryobiology* 1990; **27**: 247.
- Fahy GM, Levy DI, Ali SE. Some emerging principles underlying the physical properties, biological actions, and utility of vitrification solutions. *Cryobiology* 1987; **24**: 196.
- Pegg DE, Wusteman MC, Boylan S. Fractures in cryopreserved elastic arteries. *Cryobiology* 1997; **34**: 183.
- Hunt CJ, Song YC, Bateson EA, Pegg DE. Fractures in cryopreserved arteries. *Cryobiology* 1994; **31**: 506.
- Wassenaar C, Wijsmuller EG, Van Herwerden LA, Aghai Z, Van Tricht CL, Bos E. Cracks in cryopreserved aortic allografts and rapid thawing. *Ann Thorac Surg* 1995; **60**(Suppl. 2): S165.
- Fischer EI, Armentano RL, Pessana FM, *et al.* Endothelium-dependent arterial wall tone elasticity modulated by blood viscosity. *Am J Physiol Heart Circ Physiol* 2002; **282**: H389.
- Gamero LG, Armentano RL, Barra JG, Simon A, Levenson J. Identification of arterial wall dynamics in conscious dogs. *Exp Physiol* 2001; **86**: 519.
- Ljung L. *System Identification. Theory for the User*, 2nd edn. Upper Saddle River, NJ: Prentice Hall, 1999.
- Akaike H. Fitting autoregressive models for prediction. *Ann Inst Stat Math* 1969; **21**: 243.
- Peterson LH, Jensen RE, Parnell J. Mechanical properties of arteries in vivo. *Circ Res* 1960; **8**: 622.
- Varanasi KK. Models of damped systems. On the design of a precision machine for closed-loop performance. MS Thesis, Massachusetts, Cambridge: Massachusetts Institute of Technology, 2002.
- Mavrilas D, Tsapikouni T. Dynamic mechanical properties of arterial and venous grafts used in coronary bypass surgery. *J Mech Med Biol* 2002; **2**: 1.
- Silver FH, Snowhill PB, Foran DJ. Mechanical behavior of vessel wall: a comparative study of aorta, vena cava, and carotid artery. *Ann Biomed Eng* 2003; **31**: 793.
- Vischjager M, Van Gulik TM, Van Marle J, Pfaffendorf M, Jacobs MJ. Function of cryopreserved arterial allografts

- under immunosuppressive protection with cyclosporine A. *J Vasc Surg* 1996; **24**: 876.
31. Adham M, Gournier JP, Favre JP, et al. Mechanical characteristics of fresh and frozen human descending thoracic aorta. *J Surg Res* 1996; **64**: 32.
 32. Karlsson JO, Toner M. Long-term storage of tissues by cryopreservation: critical issues. *Biomaterials* 1996; **17**: 243.
 33. Rendal Vazquez ME, Rodriguez Cabarcos M, Martinez Santos MV, et al. Functional assessment of cryopreserved human aortas for pharmaceutical research. *Cell Tissue Bank* 2004; **5**: 119.
 34. Bujan J, Pascual G, Lopez R, et al. Gradual thawing improves the preservation of cryopreserved arteries. *Cryobiology* 2001; **42**: 256.
 35. Blondel W, Lehalle B, Maurice G, Wang X, Stoltz JF. Rheological properties of fresh and cryopreserved human arteries tested in vitro. *Rheologica Acta* 2000; **39**: 461.
 36. Pontrelli G, Rossoni E. Numerical modelling of the pressure wave propagation in the arterial flow. *Int J Numer Meth Fluids* 2003; **43**: 651.
 37. Shadwick RE. Mechanical design in arteries. *J Exp Biol* 1999; **202**: 3305.
 38. Wells SM, Langille BL, Lee JM, Adamson SL. Determinants of mechanical properties in the developing ovine thoracic aorta. *Am J Physiol* 1999; **277**: H1385.
 39. Silver FH, Horvath I, Foran DJ. Viscoelasticity of the vessel wall: the role of collagen and elastic fibers. *Crit Rev Biomed Eng* 2001; **29**: 279.
 40. Silver FH, Ebrahimi A, Snowhill PB. Viscoelastic properties of self-assembled type I collagen fibers: molecular basis of elastic and viscous behaviors. *Connect Tissue Res* 2002; **43**: 569.
 41. Taylor MG. Wave transmission through an assembly of randomly branching elastic tubes. *Biophys J* 1966; **6**: 697.
 42. Langerak SE, Groenink M, van der Wall EE, et al. Impact of current cryopreservation procedures on mechanical and functional properties of human aortic homografts. *Transpl Int* 2001; **14**: 248.